J. Fluid Mech. (1969), *vol.* 37, *part* 4, *pp.* 625–642
Printed in Great Britain

The calculation of three-dimensional turbulent boundary layers in incompressible flow

By J. F. NASH
Lockheed Georgia Research Laboratory, Marietta, Georgia

(Received 24 October 1968 and in revised form 3 February 1969)

A method is described for calculating the development of a three-dimensional turbulent boundary layer, over a flat or developable surface, in incompressible flow. The method involves the numerical integration of the equations of motion by an explicit finite-difference method. The shear stress is determined by a parallel integration of the turbulent energy equation modified by the inclusion of empirical functions of a form which has proved successful in two dimensions, and the additional assumption is made that the turbulent shear stress acts in the direction of the rate of strain of the mean motion. The treatment of the turbulent energy equation follows closely the work of Bradshaw, Ferriss & Atwell (1967) in two dimensions.

Comparison with experiment is found to be substantially more difficult than in two dimensions. Particular difficulty is encountered in translating the recorded details of the experiment into boundary conditions for the calculation. The comparisons submitted here give some indication that the method as a whole performs satisfactorily, but they do not provide a definitive assessment of the validity of the basic assumptions. A plea is made for an experiment to supply data in a suitable form for making a more careful assessment of methods of this type.

1. Introduction

Three-dimensional turbulent boundary layers are so much more common in practice than two-dimensional ones that the amount of research effort which has been, and continues to be, expended on the latter problem seems disproportionately large. Few attempts have been made to study three-dimensional boundary layers either experimentally or theoretically; and, as far as the development of calculation methods is concerned, the great majority of investigators have never ventured into three dimensions, presumably being deterred by the larger number of velocity and shear stress components that have to be considered.

The small amount of published theoretical work has been confined almost exclusively to the application of integral methods and to the study of mean velocity profiles. However, this latter study has shown that the profile shapes (especially the crossflow profile shapes) are too complicated to be represented adequately by a small number of parameters (e.g. Joubert, Perry & Brown 1967; Klinksiek & Pierce, unpublished), and therefore it seems doubtful whether a sufficiently flexible integral method can be constructed on the basis of a small

number of integral equations. One involving a larger number of integral equations would offer few advantages, if any, but many disadvantages compared with a differential method. Integral methods are losing popularity in two dimensions, and they are even less attractive in three.

One of the current fears about the numerical approach is that it will make excessive machine demands. However, this does not appear to be so, and the present work should demonstrate that meaningful calculations can be performed on computers of modest size and at modest cost. Another fear is that the assumptions regarding the turbulence are more exposed in a finite-difference method, and that suitable assumptions cannot yet be made with enough confidence. In reply to this objection, it is hoped that the present work shows that techniques are currently available for estimating the magnitude and direction of the turbulent shear stress, and that these techniques are at least sufficiently promising to form the basis for future refinement. In any case, the consequences of the various assumptions can be assessed more readily than is possible with the type of global assumptions common in integral methods.

In the present work, the differential equations of motion (the equations expressing the momentum balance in the two orthogonal directions parallel to the wall), and the continuity equation, are integrated numerically using an explicit finite-difference method. The shear stress is determined from the empirically modified turbulent energy equation, following the work of Townsend (1955), Bradshaw *et al.* (1967) and McDonald (1968). As in two dimensions, the assumption is made that the magnitude of the shear stress is directly proportional to the turbulent intensity, and the additional assumption is made that the shear stress acts in the direction of the maximum rate of strain of the mean motion. These assumptions are regarded as being of a provisional nature and, when it appears to be necessary, the overall method can be updated to embrace a more sophisticated flow model with little difficulty. The relevant assumptions are discussed in more detail in § 3.

The numerical scheme is described in § 4, and comparisons with experiment are presented in § 5.

The present method is restricted to incompressible flows and also restricted to flows over flat surfaces (or developable surfaces of large radius.) In principle the extension to more general geometries requires only the inclusion of the curvature terms in the equations of motion, so long as the body radii remain large compared with the boundary-layer thickness.

2. Basic equations

A regular co-ordinate system (x, y, z) is chosen with y measured normal to the surface (figure 1). The flow is assumed to be incompressible and non-time-dependent, in the mean.

If the normal-stress terms are neglected, the two momentum equations for the mean motion not too close to the wall are

$$\frac{DU}{Dt} + \frac{1}{\rho}\frac{\partial p}{\partial x} + \frac{\partial}{\partial y}(\overline{uv}) = 0, \tag{1}$$

$$\frac{DW}{Dt}+\frac{1}{\rho}\frac{\partial p}{\partial z}+\frac{\partial}{\partial y}(\overline{vw})=0, \tag{2}$$

where

$$\frac{D}{Dt}=U\frac{\partial}{\partial x}+V\frac{\partial}{\partial y}+W\frac{\partial}{\partial z}, \tag{3}$$

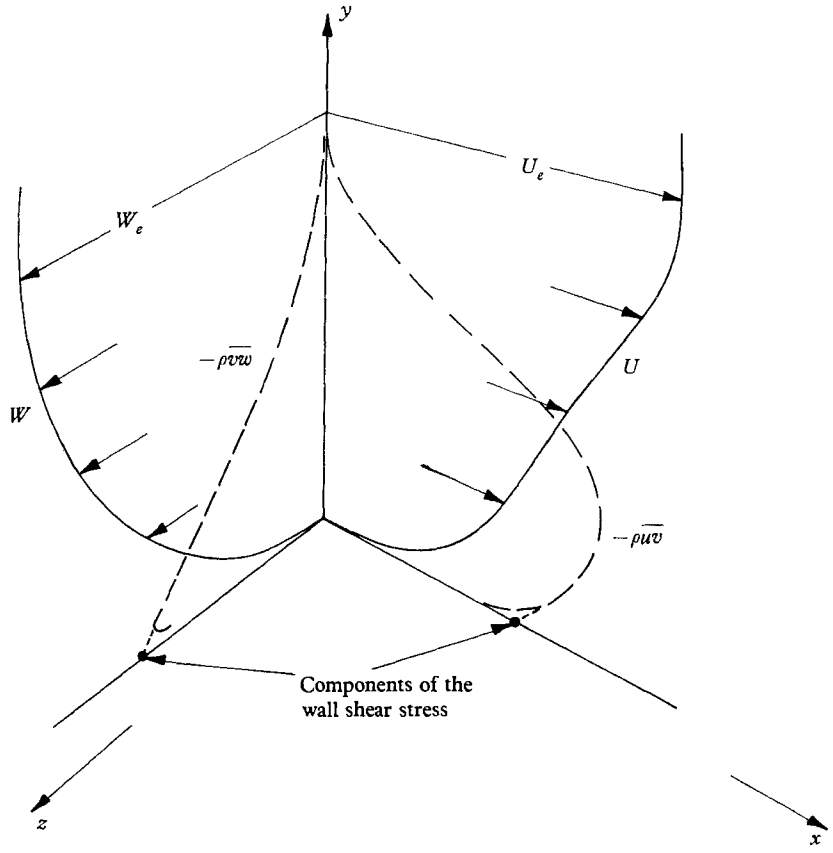

FIGURE 1. Schematic diagram showing the mean velocity and shear stress profiles.

and the continuity equation is

$$\frac{\partial U}{\partial x}+\frac{\partial V}{\partial y}+\frac{\partial W}{\partial z}=0. \tag{4}$$

U, V, W are the mean velocity components, and u, v, w the fluctuating velocity components, in the x, y, z directions respectively; p is the static pressure and ρ the density.

The kinetic-energy equation for the fluctuating velocity components (the turbulent energy equation) can be written

$$\underset{\text{Advection}}{\frac{D}{Dt}\left(\frac{\overline{q^2}}{2}\right)}+\underset{\text{Production}}{\left(\overline{uv}\frac{\partial U}{\partial y}+\overline{vw}\frac{\partial W}{\partial y}\right)}+\underset{\text{Diffusion}}{\frac{\partial}{\partial y}\overline{\left\{v\left(\frac{p'}{\rho}+\frac{q^2}{2}\right)\right\}}}+\underset{\text{Dissipation}}{\epsilon}=0, \tag{5}$$

where p' is the fluctuating component of the static pressure; a bar denotes the time average. The resultant fluctuating velocity is

$$\overline{q^2} = \overline{u^2} + \overline{v^2} + \overline{w^2}. \tag{6}$$

As before, the viscous and normal-stress terms have been neglected.

In the above system of equations there are more unknowns than relations, and empirical information must be introduced to make the system determinate. Here, the empiricism is introduced by modelling the advection, diffusion and dissipation terms in the turbulent energy equation.

3. Assumptions

Following the work of Townsend (1955), Bradshaw *et al.* (1967) and McDonald (1968) in two dimensions, three assumptions can be written down at once.

$$\{(\overline{uv})^2 + (\overline{vw})^2\}^{\frac{1}{2}} = a_1 \overline{q^2}, \tag{7}$$

$$\overline{v\left(\frac{p'}{\rho} + \frac{q^2}{2}\right)} = \frac{1}{Q_e}(\overline{q^2})_{\max}(\overline{q^2}) \cdot a_2\left(\frac{y}{\delta}\right), \tag{8}$$

$$\epsilon = (\overline{q^2})^{\frac{3}{2}}/L\left(\frac{y}{\delta}\right), \tag{9}$$

where a_1 is the ratio of the magnitude of the shear stress to the turbulent intensity, a_2 is a turbulent diffusion parameter, Q is the resultant mean velocity ($Q^2 = U^2 + W^2$ to the boundary-layer approximation), and L is the dissipation length; subscript e denotes conditions at the edge of the boundary layer, and the boundary-layer thickness is defined as $\delta = (y)_Q$ for $Q = 0{\cdot}995 Q_e$. The first states that the magnitude of the shear stress is proportional to the turbulent intensity *via* a constant a_1, which is taken equal to 0·15. The second expresses the diffusion term (to the boundary-layer approximation only the diffusion normal to the wall is significant) as a function of the local intensity and the maximum intensity at the particular x, z station. The form of this expression emphasizes the aspect of bulk diffusion, and the value of the 'diffusion coefficient', a_2, at the edge of the boundary layer is chosen to impose the correct two-dimensional entrainment rate (see Bradshaw *et al.* 1967). The use of the same expression in three dimensions is felt to be justified because diffusion is only important near the outer edge of the boundary layer, where the velocity and shear-stress profiles are approximately collateral. The third assumption, (9), implies that the dissipating eddies are approximately isotropic, but is otherwise uncontentious until L is specified.

The diffusion coefficient and the dissipation length are assumed to be universal functions of y/δ (figure 2), and the form of the functions is taken to be the same as proved successful in two dimensions (Nash 1968). The use of δ as the scaling length for quantities related to the turbulence (especially for L) is again analogous to the work in two dimensions. However, the justification of its use becomes more questionable in a three-dimensional boundary layer because of the larger range of values of $\partial\delta/\partial x$ (and $\partial\delta/\partial z$) made possible by lateral flow divergence or convergence. An experimental study is required to investigate the rate of increase of eddy size in a boundary layer whose thickness is rapidly increasing or decreasing.

The suspicion that this effect may be significant is strengthened by the difficulties that have been encountered (elsewhere) in predicting the wall shear stress in the boundary layer on a waisted body of revolution, measured by Winter, Smith & Rotta (1965).

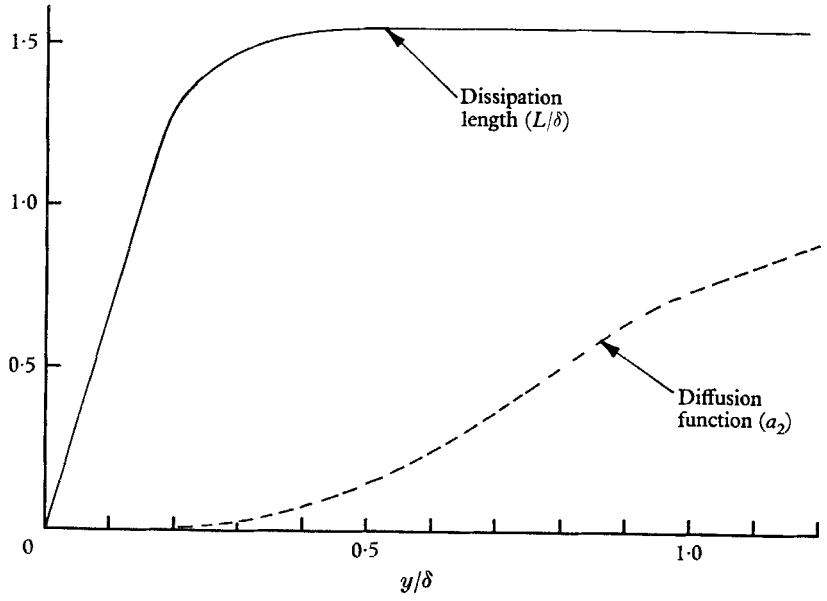

FIGURE 2. Empirical functions.

The assumption that the magnitude of the shear stress is proportional to the turbulent intensity is a consequence of Townsend's structural–equilibrium hypothesis, and it can be expected to be valid away from the edges of the turbulent region and (at least in two dimensions) away from regions where the mean-velocity gradient changes sign. For practical purposes it appears to be an adequate approximation to assume that it holds more generally (Bradshaw *et al.* 1967). Objections which can be made about the validity of this assumption near mean-velocity maxima are of little practical significance, since the shear stress is usually small in those cases anyway.

The structural-equilibrium hypothesis asserts that if a mean-velocity gradient is suddenly imposed on a field of turbulence, the turbulence becomes fully strained, i.e. reaches an asymptotic degree of anisotropy, in a time which is short compared to the time taken to reach energy (and, by implication, shear-stress) equilibrium. Very recently, the validity of Townsend's hypothesis has been questioned on the basis of experimental results (Tucker & Reynolds 1968). However, the observed discrepancies do not appear to be so serious as to place the corresponding assumptions, involved here, on a lower order of credibility than the remaining assumptions in this work. Another assertion consistent with the hypothesis is that, in three dimensions, the direction of the shear stress responds to a change of the mean velocity gradient more quickly than does its magnitude. The precise relationship between the various time scales is likely to remain a

subject of controversy for some time, but here the provisional assumption is made that the directional response-time is short, and therefore that the shear stress acts approximately in the direction of the maximum rate of strain of the mean flow

$$\overline{uv}/(\partial U/\partial y) = \overline{vw}/(\partial W/\partial y), \tag{10}$$

where both of these ratios are negative. Equation 10 is consistent with the concept of a scalar eddy viscosity, although the present method does not, of course, imply that the value of this scalar can be prescribed in advance.

The above system of equations approximate to the physical situation only in the fully turbulent part of the boundary layer. The exclusion of the viscous terms precludes their application to the sublayer and blending region; indeed the author is unaware of any method for solving the flow in the blending region, unless empirical modifications to mixing-length or eddy-viscosity profiles are regarded as 'solutions'.

To overcome this difficulty the numerical solution is matched to the universal inner law at some convenient, small distance from the wall: in practice the first mesh point away from the surface. The inner law is assumed to be applicable to three-dimensional flows when used to relate the magnitude of the wall shear stress and the absolute mean velocity. The first mesh point is usually taken at about $y/\delta = 0{\cdot}03$, and probably this is sufficiently close to the wall for it to be unnecessary to incorporate the modifications to the inner law suggested by Perry & Joubert (1965). The matching point is assumed to lie in the logarithmic region regardless of the value of $y(\tau_w/\rho)^{\frac{1}{2}}/\nu$, where τ_w denotes the resultant wall shear stress and ν the kinematic viscosity; this is consistent with the nature of the equations which have a logarithmic solution for small y.

4. Method of solution

The integration domain

The problem consists of integrating (1), (2), (4) and (5) simultaneously, incorporating the various empirical assumptions and giving the appropriate boundary conditions.

In the present work, the equations are integrated in a three-dimensional domain bounded in the y-direction by the wall and a surface a short distance beyond the 'edge' of the boundary-layer (figure 3), and in the z-direction in some convenient manner for the particular geometry (figure 4). The domain can, in principle, be semi-infinite in the x-direction, in which the calculation proceeds. The co-ordinate system is not forced to coincide with the external streamline pattern, nor it is necessary to know where the streamlines are at the outset. It is required to specify only the pressure distribution, and the only restriction is that the U-component of velocity be positive everywhere in the domain. There is no restriction to small 'crossflows'.

A rectangular mesh is used, but the collocation points in the y-direction are redistributed after each x-step; this is done, partly to allow for an increase (or decrease) in the maximum boundary-layer thickness at that x-station, and partly as an aid to stability. The mesh is staggered as shown in figure 3. Typically,

between 12 and 15 points are taken in the y-direction. The z-step can be chosen to suit the magnitude of the gradients in the z-direction; the maximum number of z-stations used so far in this work has been 21. The x-step is typically 0·2 to

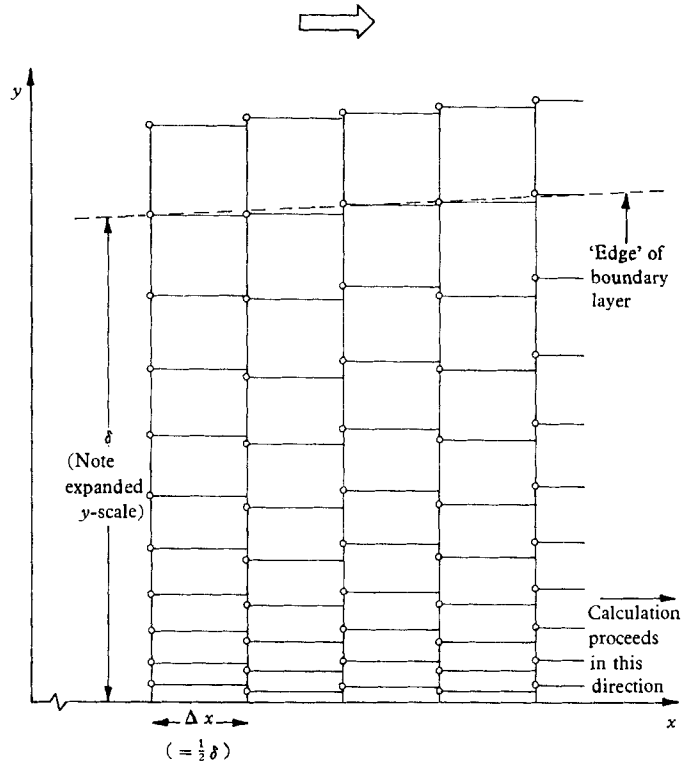

FIGURE 3. Mesh pattern (x, y plane): cross-section of integration domain.

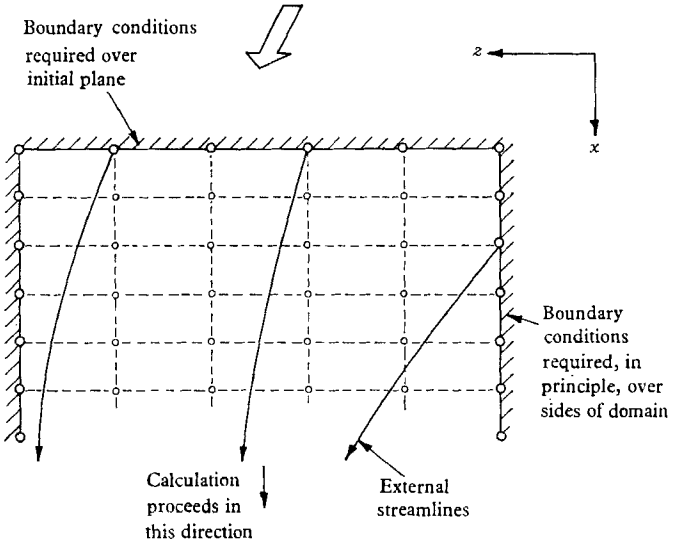

FIGURE 4. Mesh pattern (x, z plane): 'plan view' of integration domain.

0·5 times the *minimum* boundary-layer thickness at that x-station, subject to stability restrictions on the maximum value of $\Delta x/\Delta z$† (for mesh size Δx, Δy, Δz).

Calculation procedure

The calculation proceeds in the x-direction, values of all the dependent variables being determined over successive planes: x = constant. Thus at each x-station, a row of mean velocity and shear stress profiles is calculated.

The two momentum equations, (1) and (2), and the modified turbulent energy equation, (5), (6) and (10), are used to determine the values of $\partial U/\partial x$, $\partial W/\partial x$ and $\partial(\overline{q^2})/\partial x$, respectively, at a given x-plane, in terms of the various flow parameters, at that plane, and their y- and z-derivatives. Values of U, W and $\overline{q^2}$ are then found at the end of the x-interval by a straightforward explicit, forward-difference scheme.

After the collocation points are redistributed, as shown in figure 3, new values of U, W and $\overline{q^2}$ are found from the previously calculated ones by interpolation. The interpolation process has a stabilizing influence on the computation at the expense of little loss of precision. The stability and accuracy of a two-dimensional version of this numerical scheme are discussed by Nash (1968). It must be emphasized that the stability criteria for parabolic equations, for instance, those describing the laminar boundary layer, are irrelevant to the present problem since the equations form a hyperbolic system; this is true even in two dimensions as a result of the particular form of the diffusion term in the present model (Bradshaw *et al.* 1967; Nash 1968).

The integration is carried out for all the mesh points over the y-z plane, down to the first row away from the surface.

The values of V over the forward plane are found from the following expression, which can be derived by eliminating $\partial U/\partial x$ between the x-momentum equation and the continuity equation

$$V = -U\int_0^y \left\{\frac{1}{U^2}\frac{DU}{Dt} + \frac{\partial}{\partial z}\left(\frac{W}{U}\right)\right\} dy. \tag{11}$$

The magnitudes of the wall shear stress vectors at the forward station are found from the mean velocities at the first row of mesh points, using the simple inner-law relation

$$Q = \frac{1}{\kappa}\left(\frac{\tau_w}{\rho}\right)^{\frac{1}{2}}\left[\ln\left\{\frac{y}{\nu}\left(\frac{\tau_w}{\rho}\right)^{\frac{1}{2}}\right\} + C\right], \tag{12}$$

where Q is the resultant mean velocity; the following values have been assigned to the constants:

$$\left.\begin{aligned}\kappa &= 0{\cdot}4,\\ C &= 2{\cdot}0.\end{aligned}\right\} \tag{13}$$

The direction of the wall shear stress vectors is found by extrapolating the direction of the mean velocity vectors from the first few mesh points away from the surface. It does not appear to be sufficiently accurate to assume that the mean velocity profiles are collateral between the wall and the first mesh point, although to assume that they are not strictly undermines the validity of (12).

† The appropriate Courant–Friedrichs–Levy condition is that $\Delta x/\Delta z$ must be less than $|U/W|$.

Boundary conditions

Values of U, W and $\overline{q^2}$ are required to be known over the initial plane; these data correspond to a *row* of velocity and shear-stress profiles in place of the single pair of profiles required in a two-dimensional calculation. The initial shear-stress profiles are rarely known, and usually they must be estimated from the velocity profiles using, say, mixing-length theory. This was necessary in the present work, but in the comparisons with experiment shown below (§ 5), the possible errors thus introduced have been minimized by allowing the boundary layer some initial length to settle down before reaching the matching station. Fortunately, unless the early part of the run is a region of large adverse pressure gradient, the solution is fairly insensitive to the initial shear stresses.

At the upper surface of the domain the appropriate boundary conditions are

$$\left.\begin{aligned} \frac{\partial U}{\partial y} = \frac{\partial W}{\partial y} = \frac{\partial}{\partial y}(\overline{q^2}) = 0, \\ \overline{q^2} = 0, \end{aligned}\right\} \tag{14}$$

$$\frac{\partial U}{\partial z} - \frac{\partial W}{\partial x} = 0. \tag{15}$$

The condition of irrotationality in the external flow, (15), places a restriction on the generality of the pressure field which can be imposed. It will be noted that if the pressure distribution is specified over the domain, and also the values of U_e and W_e on the boundary, then in general it is possible to construct flows which do not satisfy this condition.† Care must be taken to ensure that the flows, for which calculations are being performed, are physically relevant.

The boundary conditions at the wall are taken care of by matching the numerical solution to the universal inner law.

In general, boundary conditions are also required along the sides of the integration domain, although in most cases it is practically impossible to specify them. In the present calculations, the side boundary conditions have been invented by extrapolating outwards from within the domain. Values of U, W and $\overline{q^2}$ were found by linear extrapolation from the first two mesh points from the edge of the domain. In cases where fluid is flowing into the domain through a particular side, this procedure creates a potentially unstable region, which spreads inwards from that side as the calculation proceeds downstream, bounded (in principle) by the stream surface originating from the upstream 'corner' of the domain. If fluid is leaving the domain through a particular side, conditions on that boundary are, in principle, determined by conditions inside the domain, and the extrapolation process has rather more justification.

† Some of the three-dimensional laminar boundary layers referred to in chapter 8 of Rosenhead (1963) have this property.

Machine time

The method was programmed in FORTRAN 4, and the computations were performed on an IBM 360-50 machine. The running time for the calculation of Hornung & Joubert's (1963) boundary layer (§ 5) was of order 5 min.

5. Comparison with experiment

Making comparisons between theory and experiment for three-dimensional turbulent boundary layers, and interpreting the degree of correlation achieved, is substantially more difficult than in two dimensions. In most cases a computer program has to be set up for each flow situation, incorporating as close an approximation to the boundary conditions as can reasonably be made from the recorded experimental conditions. The task of interpreting the experimental conditions is complicated by the unknown sensitivity of both the real flow and the calculation method to small departures from the true boundary conditions.

Initially it was hoped to include comparisons with four sets of experimental data, but two of these were discarded at a late stage in the work. Comparisons with Francis & Pierce's (1967) data were discarded, because it was found that the boundary layer in their curved channel was dominated by the effects of the corner flow at the junction of the side walls and the floor of the channel, and these effects could not be taken into account properly in the calculations. Comparisons with Cumpsty's (1967) data on the attachment-line boundary layers were not used, because certain discrepancies between theory and experiment appeared to arise directly from the low Reynolds numbers of the tests; the value of R_θ the Reynolds number based on momentum thickness all lie below 800. It was felt that comparisons with data at low Reynolds numbers could better form the subject of a separate study. The two remaining sets of comparisons will be presented in detail.

Cumpsty (unpublished)

These data relate to the boundary layer on the rear of a 61° swept wing (figure 5); the wing was of 18 in. chord (measured normal to the leading edge) and completely spanned a 48 in. wind-tunnel test section. Measurements of the mean velocity profiles were made between the line of minimum pressure and the separation line. Two chordwise pressure distributions, measured at spanwise stations about two chord-lengths apart, differed by an amount which varied, with chordwise position, between extremes of zero and 0·08 times the free-stream dynamic pressure ($\frac{1}{2}\rho Q_\infty^2$), where Q_∞ denotes the value of Q in the free stream at infinity.

The calculations were started 3·5 in. upstream of the minimum-pressure line (designated $x = 0$), and the predicted and measured values of δ were matched at $x = 0$. It was found that, owing to the strong negative pressure gradient upstream of the matching station, the solution was insensitive to the precise form of the velocity profiles at the initial station. Comparisons with the measured mean velocity profiles are presented in figures 6–8 for the stations A–C, shown in figure 5, which correspond to $x = 5{\cdot}6$, 7·7 and 9·8 in. respectively. The profiles

are plotted (although they were not calculated in this way) in terms of 'streamwise' and 'crossflow' components, using the commonly accepted definitions. All velocities are made dimensionless by dividing by the magnitude of the velocity vector at the edge of the boundary layer. Two sets of calculations are submitted.

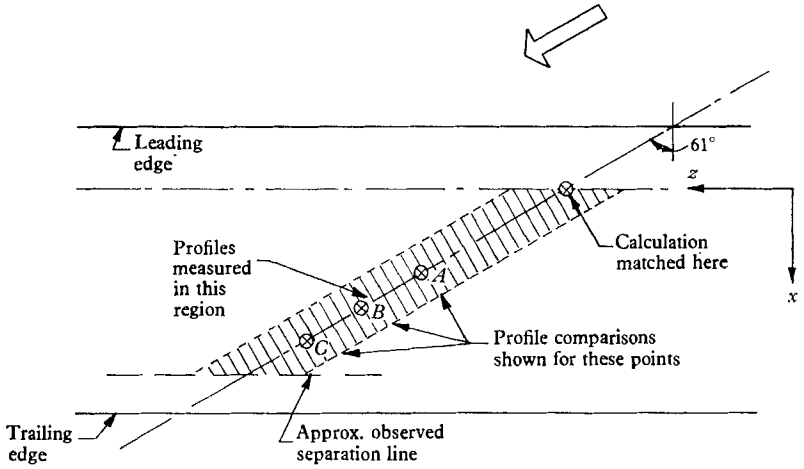

FIGURE 5. Cumpsty's flow over the rear of a swept wing.

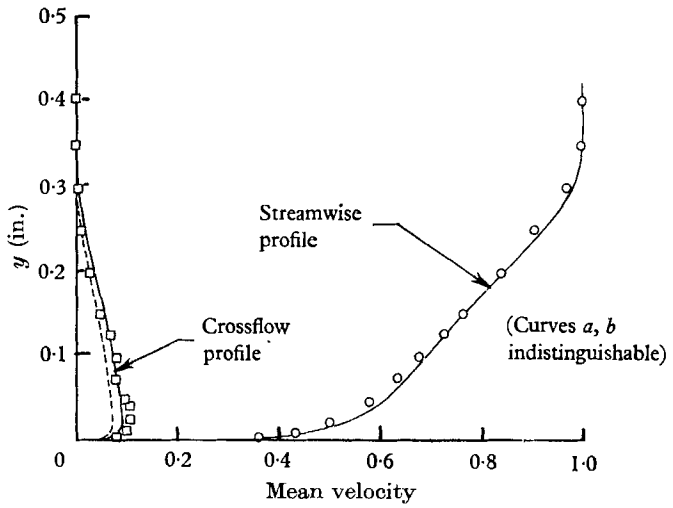

FIGURE 6. Cumpsty: mean velocity profile, station A ($x = 5{\cdot}6$ in.).
Theory: — — —, a; ———, b; Experiment: ○, □.

In calculation 'a' it was assumed that the flow corresponded to that over an infinite yawed wing, i.e. with all derivatives in the z-direction equal to zero. Calculations for infinite swept wings are quasi-two-dimensional, and need be done for one z-station only (i.e. only a two-dimensional mesh is required). This calculation failed to predict either the correct rate of increase of boundary-layer thickness with x or the correct development of the crossflow profile; at the last station (figure 8) δ is underestimated by 25 %, and the maximum crossflow

velocity by 60 %. Also, the flow was predicted to remain attached over the whole chord, whereas separation was observed experimentally.

These discrepancies are larger than can reasonably be attributed to inadequacies of the flow model. Some calculations were done in which large, arbitrary changes were made to the empirical functions, but even halving the dissipation

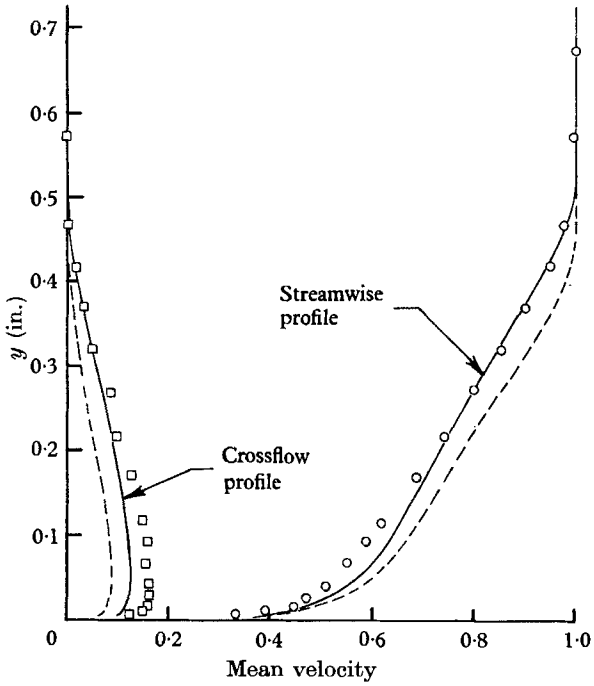

FIGURE 7. Cumpsty: mean velocity profile, station B (x = 7·7 in.).
Theory: — — —, a; ———, b. Experiment: ○, □.

length in the outer part of the boundary layer failed to bring theory and experiment much closer together. Nor can the discrepancies be attributed to additional flow convergence, i.e. additional to that normally associated with the curvature of the external streamlines on an infinite swept wing. By postulating a sufficiently large additional convergence, it was possible to match the variation of δ with x, but the shape of the velocity profiles remained essentially unaltered.

Some subsequent calculations were done to examine the effect of including a spanwise pressure gradient. These calculations required a three-dimensional mesh. The curves designated 'b' in figures 6–8 show the effect produced by a uniform gradient equal to twice that formed by dividing the *maximum* difference in pressure between the two spanwise measuring stations by the distance between them. This calculation is in considerably better agreement with experiment than 'a'. The streamwise and crossflow profiles are now predicted tolerably well and separation is predicted to occur a short distance downstream of station C (separation being defined here as the condition where the chordwise component of the wall shear stress falls to zero). It is difficult to claim more than that the postulation of such a spanwise pressure gradient offers a means of reconciling

theory and experiment, and that there is evidence of some spanwise pressure variations from the recorded measurements. But in any event the calculation draws attention to the sensitivity of this type of flow to small spanwise gradients, and to the difficulty of setting up an experiment to represent infinite-swept-wing conditions.

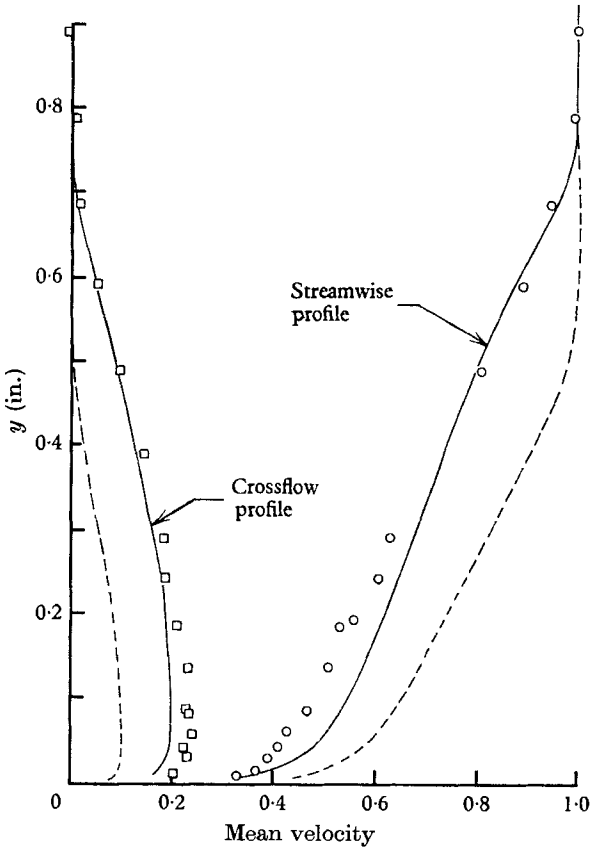

FIGURE 8. Cumpsty: mean velocity profile, station C (x = 9·8 in.).

Hornung & Joubert (1963)

These data relate to the flow over a flat plate approaching a circular cylinder, of 22 in. diameter, standing with its axis normal to the plate (figure 9). The cylinder had a fairing on its leeward side, but the pressure distribution ahead of it corresponded closely to that given by two-dimensional potential flow past an isolated cylinder (the plate forms a stream surface of the potential flow), and this potential-flow pressure distribution was used in the calculations. In the calculations the plate was regarded as being semi-infinite, and the integration domain extended from 18 in. on one side of the axis of symmetry to 36 in. on the other side.

The calculations were started 60 in. upstream of the cylinder, and at the initial station the mean velocity profiles were assumed to be of uniform thickness, collateral, and of 'flat-plate' form, but with the appropriate velocity vector

(according to the potential flow) at their outer edges. The thickness of the initial boundary layers was adjusted so as to match the measured value of δ at a point on the axis 14·5 in. upstream of the cylinder.

Comparisons with the measured mean velocity profiles are shown in figures 10–12 for stations A–C (see figure 9), which correspond to runs 14, 8 and 23, respectively, in the original paper. As before, the profiles are plotted in terms of their streamwise and crossflow components. Two sets of calculations are shown.

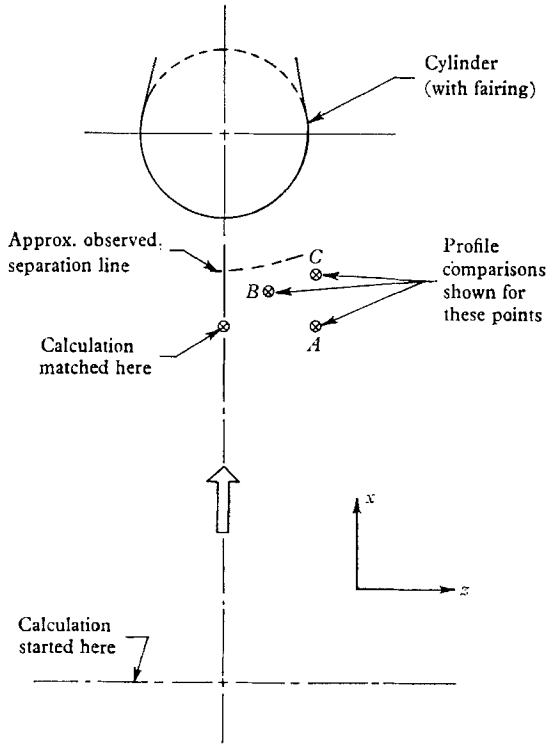

FIGURE 9. Hornung & Joubert's flow approaching a circular cylinder.

In calculation 'a' the unmodified potential-flow pressure distribution was used. The results are in fair agreement with experiment except that there is a tendency to underestimate the crossflow velocities near the wall at stations A and C (figures 10 and 12), particularly the latter.

Part of the discrepancy can be traced to a slight asymmetry in the original experiment; the mean velocity profiles on the axis have a small crossflow component. In order to simulate this in the theory, a second calculation. 'b' ,was performed, in which a small, uniform lateral pressure gradient was superimposed on the potential-flow distribution (with appropriate changes in the initial velocities to preserve the irrotationality of the external flow). The magnitude of the additional pressure gradient was chosen to reproduce the order of crossflow velocities at the matching station. Calculation 'b' is in better agreement with the measurements at station C but a discrepancy remains. This may be due to inaccuracies in representing the pressure field.

The general shape of the streamwise velocity profiles is predicted well, especially the change in 'fullness' between that at station B (figure 12) and the other two. There is a tendency to underestimate the boundary-layer thickness at stations A and C but not at B, indicating that the development of the flow in the z-direction has not been predicted sufficiently well. Again, this may be the

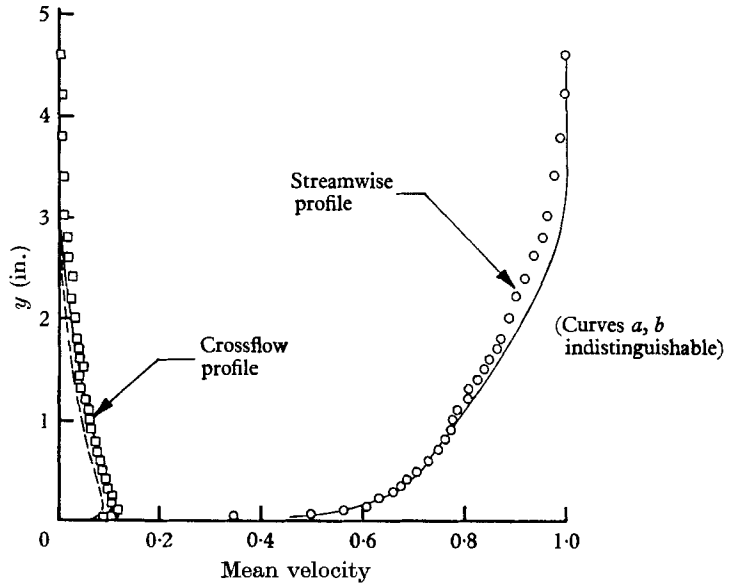

FIGURE 10. Hornung & Joubert: mean velocity profile, station A (run 14). Theory: — — —, a; ———, b. Experiment: ○, □.

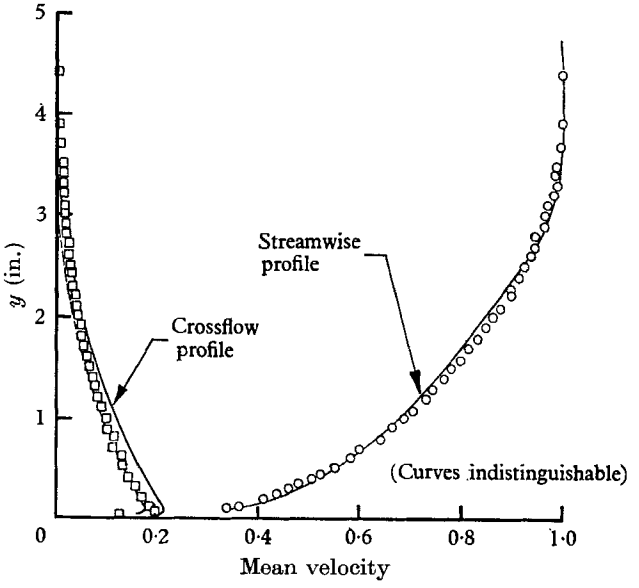

FIGURE 11. Hornung & Joubert: mean velocity profile, station B (run 8). Theory: — — —, a; ———, b. Experiment: ○, □.

result of the assumption that the pressure field could be approximated by that corresponding to potential flow.

It will be noted that the crossflow profiles in Hornung & Joubert's boundary layer are characteristically different from those in Cumpsty's. In the former case the profiles are essentially hollow, presumably a result of the strong, quasi-inviscid yawing of the flow, whereas in the latter case the profiles are 'full',

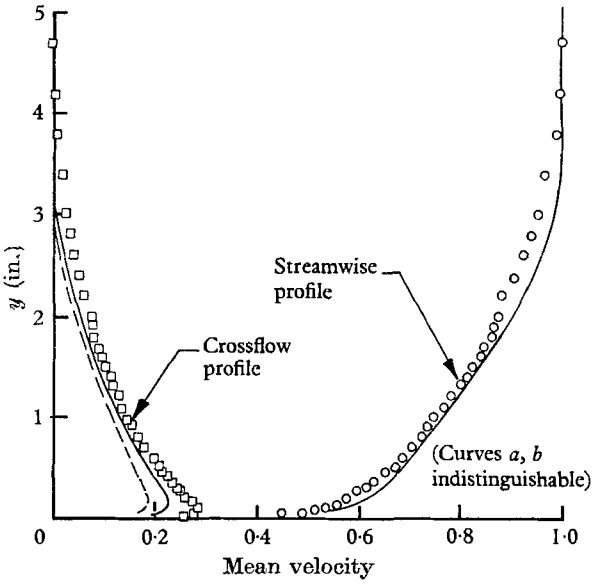

FIGURE 12. Hornung & Joubert: mean velocity profile, station C (run 23). Theory: — — —, a; ———, b. Experiment ○, □.

indicating the more significant role played by the shear stress. This difference in form of the profiles is predicted well by the theory. On the other hand, because Hornung & Joubert's flow was dominated by the pressure gradients, the moderate success with which their boundary layer was calculated affords little verification of the assumptions regarding the shear stress.

6. Conclusions

This work has demonstrated the feasibility of performing calculations on three-dimensional turbulent boundary layers by means of the numerical integration of the time-averaged equations of motion. The method is more general than previous ones: it is not restricted to boundary layers with small crossflows, to flows without points of inflexion in the external streamlines, or to quasi-two-dimensional flows, such as those past infinite swept cylinders. Moreover, it would appear to have considerable development potential. The machine demands of the method are not excessive, and useful calculations can be performed on computers of modest size.

The magnitude of the shear-stress vector is determined from the integration of the turbulent energy equation, modified by the inclusion of empirical functions.

The form of these functions has been carried over from successful studies in two dimensions, but the assumption that their form can be retained must be regarded as a potential source of uncertainty no less than the additional assumption, which has had to be made, about the direction of the shear-stress vector. There are, as yet, no suitable data for checking these individual assumptions, nor has it been possible to make a definitive assessment of the overall performance of the method.

This investigation has drawn attention to the problems involved in comparing even the mean flow development with experiment. One of the comparisons submitted here, that with Cumpsty's data, proved inconclusive, because there appeared to be a substantial effect due to a spanwise pressure gradient, the precise nature of which could not be determined from the recorded experimental data. The other comparison, with Hornung & Joubert's data, confirmed the success of the scheme for integrating the equations of motion, but shed little light on the validity of the shear-stress model, because their flow was dominated by the pressure field.

Thus, while the comparisons with experiment are encouraging, in terms of the present state of the art, the major task of determining the detailed validity of the method must await the availability of further measurements. Therefore, in addition to making the customary plea for more experimental data in general, it might be useful to plead for an experimental program aimed specifically at providing data in a suitable form for checking the validity of calculation methods of the present type. It is hoped that the major features required of such a series of measurements will emerge from this paper. Further studies of profile shapes, particularly in narrow curved channels, will add little to the further development of three-dimensional calculation methods.

The author is indebted to Dr N. A. Cumpsty, of the University of Cambridge, for supplying details of his experiment prior to their publication, and to Prof. P. N. Joubert, of the University of Melbourne, for supplying the tabulated data for the flow approaching the cylinder.

REFERENCES

BRADSHAW, P., FERRISS, D. H. & ATWELL, N. P. 1967 Calculation of boundary-layer development using the turbulent energy equation *J. Fluid Mech.* **28**, 593.

CUMPSTY, N. A. 1967 The calculation of three-dimensional turbulent boundary layers. Ph.D. Thesis, University of Cambridge.

FRANCIS, G. P. & PIERCE, F. J. 1967 An experimental study of skewed turbulent boundary layers in low speed flows. *J. Basic. Eng.* **89**, 597.

HORNUNG, H. G. & JOUBERT, P. N. 1963 The mean velocity profile in three-dimensional turbulent boundary layers. *J. Fluid Mech.* **15**, 368.

JOUBERT, P. N., PERRY, A. E. & BROWN, K. C. 1967 Critical review and current developments in three-dimensional turbulent boundary layers. *Fluid Mechanics of Internal Flows.* Amsterdam: Elsevier.

MCDONALD, H. 1968 The departure from equilibrium of turbulent boundary layers. *Aero. Quart.* **19**, 1.

NASH, J. F. 1968 A finite-difference method for the calculation of incompressible turbulent boundary layers in two dimensions. *Lockheed-Georgia Co., Rep.* ER-9655.

PERRY, A. E. & JOUBERT, P. N. 1965 A three-dimensional turbulent boundary layer. *J. Fluid Mech.* **22**, 285.

ROSENHEAD, L. (ed.) 1963 *Laminar Boundary Layers.* Oxford: Pergamon.

TOWNSEND, A. A. 1955 *The Structure of Turbulent Shear Flow.* Cambridge University Press.

TUCKER, H. J. & REYNOLDS, A. J. 1968 The distortion of turbulence by irrotational plane strain. *J. Fluid Mech.* **32**, 657.

WINTER, K. G., SMITH, K. G. & ROTTA, J. C. 1965 Turbulent boundary-layer studies on a waisted body of revolution in subsonic and supersonic flow. *Agardograph*, 97.